

Changes in seismic anisotropy at Ontake volcano: a tale of two eruptions

J.-M. Kendall *¹, T. Terakawa ², M. Savage ³, T. Kettlety ¹, D. Minifie⁴, H. Nakamichi ⁵, A. Wuestefeld ⁶

¹Department of Earth Sciences, University of Oxford, Oxford, U.K., ²Graduate School of Environmental Studies, Nagoya University, Nagoya, Japan, ³School of Geography, Environment and Earth Sciences, Victoria University of Wellington, New Zealand, ⁴School of Earth Sciences, University of Bristol, U.K., ⁵Sakurajima Volcano Research Center, Disaster Prevention Research Institute, Kyoto University, Kagoshima, Japan, ⁶NORSAR, Gunnar Randers vei 15, 2007 Kjeller, Norway

Author contributions: *Conceptualization:* J-M. Kendall, T. Terakawa, M. Savage. *Formal Analysis:* J-M. Kendall, M. Savage, T. Kettlety, D. Minifie, A. Wuestefeld. *Data provision and handling:* T. Terakawa, H. Nakamichi. *Software:* J-M. Kendall, M. Savage, T. Kettlety. *Writing – original draft:* J-M. Kendall, T. Terakawa, M. Savage. *Writing – review & editing:* All authors.

Abstract The interaction of faults, fractures, and hydromagmatic systems of volcanoes can lead to complicated stress patterns that vary over short spatial and temporal scales. Here we study stress-induced anisotropy using observations of shear-wave splitting at 12 stations across Ontake volcano, Japan. The results reveal a complicated pattern of anisotropy, indicating that the volcano perturbs the local stress field. In 2007, a minor phreatic eruption (Volcano Explosivity Index – VEI=0) occurred at Ontake, but there is little evidence of changes in splitting parameters during this eruption. In contrast, the much larger eruption of 2014 (VEI=3) shows clear temporal changes in splitting parameters following the eruption. The average background magnitude of anisotropy, as described by the delay time between the fast and slow shear wave, doubles to nearly 0.2 second at the onset of the 2014 eruption, but because the events shallow in depth the percent anisotropy increases dramatically from 3% to 20%. Contemporaneously, the polarisation of the fast shear-wave rotates towards $\sigma_{H_{max}}$. We interpret these observations in terms of basal heating of the hydrothermal system. We suggest that a lack of temporal variation in anisotropy parameters during the 2007 eruption indicates that a critical stress or crack density threshold must be overcome to exhibit a change in anisotropy, which may be indicative of a more significant eruption.

Production Editor:
Gareth Funning
Handling Editor:
Nicola Piana Agostinetti
Copy & Layout Editor:
Théa Ragon

Signed reviewer(s):
Luca De Siena

Received:
May 24, 2024

Accepted:

February 23, 2025

Published:

April 30, 2025

Résumé L'interaction des failles, des fractures et des systèmes hydromagmatiques des volcans peut conduire à des modèles de contraintes complexes qui peuvent varier sur de courtes échelles spatiales et temporelles. Ici, nous étudions l'anisotropie induite par la contrainte à l'aide d'observations de déphasage des ondes de cisaillement effectuées à 12 stations situées sur le volcan Ontake. Les résultats révèlent un modèle compliqué d'anisotropie indiquant que le volcan perturbe le champ de contraintes local. En 2007, lors d'une éruption phréatique mineure (VEI=0) à Ontake, peu de preuves de changement dans les paramètres de déphasage sont enregistrées. En revanche, lors de l'éruption beaucoup plus importante en 2014 (VEI=3), des changements temporels clairs dans les paramètres de déphasage sont observés après l'éruption. L'amplitude de fond moyenne de l'anisotropie, décrite comme le délai entre les ondes de cisaillement rapides et lentes, double pour atteindre près de 0,2 seconde au début de l'éruption de 2014. En parallèle, la polarisation de l'onde de cisaillement rapide s'approche de $\sigma_{H_{max}}$. Nous interprétons ces observations en termes de réchauffement basal du système hydrothermal. L'absence de variation temporelle des paramètres d'anisotropie lors de l'éruption de 2007 indique qu'un seuil critique de contrainte ou de densité de fissure doit être surmonté pour présenter un changement d'anisotropie, qui peut indiquer une éruption plus importante.

科学的要約 火山下におけるマグマ・熱水システムは断層や亀裂のような構造を反映して発達し、短い時間スケールで局所的な応力変化をもたらす可能性がある。本研究では、御嶽山周辺域の12の観測点を対象にS波偏向異方性解析を実施し、応力に関する異方性の時間変化を調べた。解析の結果、2007年水蒸気噴火(VEI=0)の前後では、S波偏向異方性のパラメータ(S波の伝播速度が速い方向、分離した2つの波の到着時間差)の時間変化はほとんどなかった。一方、2014年水蒸気噴火(VEI=3)の前後では、これらのパラメータに顕著な時間変化が検出された。平均的な異方性の強さは、分離した2つの波の到達時間差で特徴づけられる。2014年噴火開始時には、2つの波の到着時間差は0.2秒にも達し、これは2007年噴火時の約2倍に当たる。また、本研究で解析した2014年の地震活動は2007年の地震活動に比べて浅部に集中していたため、走時に占める遅れの割合は2007年時には3%だったのに対し、2014年時には20%にも達した。また、2014年の噴火前には、S波伝播速度の速い方向は、この地域の応力場の最大水平主圧縮軸方向に平行であった。これは、地下深部の熱水活動による流体の膨張と関係があると解釈できる。

2007年噴火時に異方性の時間変化が見られなかったことから、顕著な異方性の時間変化が観測されるためには、応力状態や亀裂密度が何らかの条件を満たす必要があるに違いない。このことから、異方性の時間変化は、規模の大きい噴火において検出されるものなのかもしれない。しかし、本研究で解析した2007年の地震活動の多くは山麓の地震活動で、2014年のような火山直下の地震活動ではない。このため、2007年の解析では、火山直下の異方性の時間変化をうまくとらえられなかった可能性は否定できない。

Non-technical summary Seismic monitoring is commonly used to provide an early warning of volcanic unrest, but unrest does not always lead to an eruption. Magma and fluid movement during unrest lead to variations in stresses, both in space and in time. In response, vertical cracks and fracture will open and close, mimicking the stress patterns. This in turn leads to directional variations in seismic velocities – or seismic anisotropy – and arguably the most diagnostic signature of such stress-induced anisotropy is the propagation of two shear waves, or shear-wave splitting. Here we consider seismic signals from two eruptions of Ontake volcano, which is on the main island of Honshū, Japan. The first eruption in 2007 shows clear spatial variations in stress-induced anisotropy, but no temporal change. In 2014 a much larger eruption occurred. Here a clear temporal change in anisotropy is observed. We interpret this in terms of added heat from deep in the volcano causing shallower water saturated fractures to expand. Our results show that monitoring of shear-wave splitting would provide a useful early warning of dangerous volcanic eruptions.

1 Introduction

Seismic monitoring is commonly used to provide an early warning of volcanic unrest, but unrest does not always lead to an eruption (McNutt, 1996). Raising false alarms can be dangerous in that it leads to complacency, and even a lack of investment in monitoring infrastructure. It is desirable to use seismic attributes that can be evaluated in real time, and ideally combined with other observables and experience, to improve probabilistic eruption forecasting (e.g., Sparks and Aspinall, 2004; Chouet and Matoza, 2013). Here, we present a study using seismic anisotropy as a diagnostic indicator of unrest, investigating two eruptive sequences from Ontake volcano in Japan – one a minor phreatic eruption and the other a much larger and deadly eruption.

Volcanoes produce a diverse range of seismic signals (McNutt, 2005) and identifying differences in these signals can be challenging (e.g., Lapins et al., 2020). They can be interpreted as a signature of stress release and fluid movement in a complex hydromagmatic plumbing system (e.g., Chouet, 1996; Neuberg, 2000). Further characterising the seismic signal, for example determining event magnitude and source mechanism, can indicate the style and magnitude of stress release (Terakawa et al., 2016). Such analyses can be time consuming, although semi-automated methods are now becoming more routine.

Seismic signals can also be used to image the volcano. Tomographic imaging with dense networks using earthquakes and ambient noise provides detailed images of volcanic structure (e.g., Koulakov et al., 2016). Attenuation studies are appealing as seismic attenuation is very sensitive to the presence of fluids (Del Pezzo et al., 2004; Hudson et al., 2023; De Siena et al., 2014). Finally, it has been suggested that observations of seismic anisotropy provide insights into the changing stress regime at depth (Miller and Savage, 2001; Gerst and Savage, 2004; Savage et al., 2010).

An effective forecasting tool needs to be applied in semi-real-time. Changes in character, rate and depth of seismicity are indications of unrest in the volcanic system and the inherently episodic nature of

magmatic processes (McNutt, 1996; Chouet and Matoza, 2013). Some national networks already locate earthquakes in near-real-time using standard automatic phase identification and location algorithms (e.g., GeoNet in New Zealand uses the SeisComp package <https://www.seiscomp.de/>, Petersen et al., 2011). A number of emerging methods are being used to identify and locate seismic events more rapidly, including machine learning methods (e.g., Malfante et al., 2018; Lapins et al., 2021).

A range of observations indicate that volcanic systems are often in a critically stressed state. For example, under certain circumstances the passage of seismic waves from large, but distant, earthquakes can be enough to trigger eruptions (e.g., Manga and Brodsky, 2006; Hamling and Kilgour, 2020). Rapid changes in source mechanism document changes in the stress state associated with dyke injection (Terakawa et al., 2016; Roman et al., 2004). Subtle changes in seismic velocity during eruption have been interpreted in terms of fluid or pore pressure changes (Wegler et al., 2006; Caudron et al., 2022). Finally, a growing number of studies indicate that seismic anisotropy is sensitive to stress changes in reservoirs (e.g., Gerst and Savage, 2004; Mroczek et al., 2019). Here we explore changes in seismic anisotropy before, during and after two eruptive sequences of Ontake volcano – one minor one in 2007 and a second more major eruption in 2014.

2 Seismic anisotropy as an indicator of cracks and fractures

Seismic anisotropy – or a directional variation in wavespeed and polarisation – can be caused by a number of factors including the crystal preferred orientation (CPO) of minerals, sub-wavelength period thin layering (PTL) of contrasting materials, or the shape preferred orientation (SPO) of inclusions (e.g., fluid filled cracks and fractures) (Savage, 1999; Kendall, 2000). In the shallow crust, the preferred alignment of cracks and fractures is an indication of stress orientation, as cracks will close in directions perpendicular to the direction of maximum horizontal stress ($\sigma_{H_{max}}$) (Crampton, 1984). As such, seismic anisotropy can be used as a proxy for

*Corresponding author: mike.kendall@earth.ox.ac.uk

stress anisotropy and fracture network development, all of which is valuable information in understanding fluid flow in shallow crustal reservoirs.

Here we assume stress-induced crack anisotropy is the dominant mechanism for anisotropy in a volcanic setting. Vertically aligned fractures produce a horizontal transverse isotropy (HTI) symmetry (i.e., a rotational invariance in seismic velocities around a horizontal symmetry axes) (see Kendall (2000) for more detail). In reality there is likely some sub-horizontal CPO, layering or alignment that would lead to a vertical transverse isotropy (VTI) fabric. The two fabrics combine to produce an orthorhombic symmetry (or monoclinic if the beds are dipping) (e.g., Kendall et al., 2007). However, an important point is that we are using sub-vertical raypaths from earthquakes that lie beneath a seismic station (to stay within the shear-wave window). Therefore, the rays are not sensitive to the VTI component of such fabric.

There is some ambiguity in the term stress-induced seismic anisotropy. From a theoretical point of view, pre-stress leads to anisotropy in the higher-order elastic constants (in other words, Hooke's law breaks down and higher-order elastic constants become important – see Dahlen, 1972), but this effect is subtle. In the shallow crust, a much more dominant mechanism is associated with sub-seismic-wavelength cracks and fractures. Stress anisotropy will close microcracks in the direction perpendicular to the direction of maximum horizontal stress. However, there is also the ambiguity in the use of the terms microcracks versus fractures. Fractures tend to occur in conjugate sets, resulting in a fast shear-wave polarisation that is some weighted average of the two orientations (e.g., Verdon et al., 2009). As we have a limited number of measurements at each station, we assume for simplicity a single set of microcracks or fractures aligned with the stress field.

The most unambiguous indicator of anisotropy is the propagation of two independent shear waves. A shear wave in an isotropic medium will split into two shear waves when it impinges on an anisotropic medium. These shear waves propagate with different speeds and orthogonal polarisations and remain independent even if the wavetrain re-enters an isotropic region. The time separation or delay time (δt) between the arrival of the two shear waves provides an integration of the effect of anisotropy along the entire raypath, which is a function of the strength of the anisotropy and how it varies over the region sampled. The polarisation of the fast shear-wave (φ) and the slow shear wave are an indication of the symmetry and orientation of the anisotropy, and hence its causative mechanism (e.g., Nur and Simmons, 1969; Verdon et al., 2009). In the case of vertically propagating shear waves in a medium where the anisotropy is due to the vertical alignment of thin cracks, φ will be aligned with the plane of the cracks and the slow shear wave will align perpendicular to the face of the cracks. With more general directions of wave propagation, the style of anisotropy is sensitive to the degree of fracture interconnectivity and the compressibility of fluids, which can be described by the fracture compliance (Schoenberg and Sayers, 1995). For example, the

pattern of anisotropy for gas-filled interconnected fractures is much simpler than that for water-filled and isolated fractures (see for example, Baird et al., 2013). Furthermore, the anisotropy can be frequency dependent, where cracks appear to be increasingly connected at low frequencies (Chapman, 1985; Al-Harrasi et al., 2010).

Crack and fracture induced anisotropy has been observed in a variety of shallow crustal reservoirs including oil and geothermal reservoirs and volcanic systems. A number of seismic industry studies using reflection seismology have been used to characterise reservoir anisotropy (see review in Tsvankin et al., 2010). Passive monitoring of seismicity (microseismicity) has shown evidence of stress controlled anisotropy in reservoirs (Wuestefeld et al., 2011; Jones et al., 2014; Teanby et al., 2004b). Similar methods apply in geothermal settings. Elkibbi and Rial (2005) detect stress-aligned fracture systems in the shallow crust under the Geysers geothermal reservoir, California. Nowacki et al. (2018) observe anisotropy due to a combination of the influence of a regional fault system and interactions with a secondary set of fractures in the vigorously active hydrothermal system of Aluto volcano in Ethiopia. Maher and Kendall (2018) interpret anisotropy as an interaction between local and regional stress fields, with a strong influence from regional fault patterns. Untangling the inherent anisotropy of the rock fabric from the stress-controlled crack or fracture anisotropy can be challenging (Johnson et al., 2011; Baird et al., 2017), and some studies have attempted to invert downhole microseismic data for both (Verdon et al., 2009). Several studies have suggested that gravitational stress from near-surface topography is important in explaining shear-wave splitting results, which can be particularly observed in large, single-cone volcanoes where patterns of fast anisotropic azimuths are radial to the caldera on the volcano's flanks (e.g., Araragi et al., 2015; Savage et al., 2015; Illsley-Kemp et al., 2017).

In addition to characterising the spatial distribution of in situ stresses, seismic anisotropy can be used to monitor stress changes in fluid-saturated rocks. A growing number of studies have shown temporal variations in seismic anisotropy in reservoirs from a variety of settings, including volcanic and petroleum. First, Miller and Savage (2001), and then Gerst and Savage (2004), successfully measured changes in seismic anisotropy before and after the 1995/6 eruption of Mt Ruapehu, New Zealand. Temporal changes in both fast orientations and delay times were observed during eruption sequences at Asama Volcano (Savage et al., 2010) and at Piton de la Fournaise volcano (Savage et al., 2015). Temporal changes in splitting parameters and attenuation were recorded before and after the October 1999 M3.6 earthquake at Mt Vesuvius, Italy (Del Pezzo et al., 2004). Most recently, temporal changes in splitting parameters were observed leading up to the 2019 Whakaari/White Island eruption in New Zealand (Mengesha et al., 2024). Valti and Crampin (2003) observe changes in splitting before earthquakes and volcanic eruptions in Iceland, and temporal changes in splitting at geothermal areas have also been observed in response to reservoir stimulation (e.g., Adelinet et al., 2015). Mroczek et al. (2019)

find changes in anisotropy related to geothermal energy production and accompanying injection of fluids. However, temporal changes are not always observed during eruptions (Johnson et al., 2010; Baird et al., 2015), or in response to geothermal production (González and Munguía, 2003).

Temporal changes in seismic anisotropy in oil and gas reservoirs have been interpreted in terms of stress transfer between faults due to either production (De Meersman et al., 2009) or even tidal loading (Teanby et al., 2004b). Hydraulic fracture stimulation will change the stress field, reactivating pre-existing fractures but also developing new fracture networks. Baird et al. (2013) and Wuestefeld et al. (2011) observe changes in anisotropy during hydraulic fracture stimulation in relatively impermeable gas bearing sedimentary rocks. Temporal changes have also been observed during CO₂ injection, which were attributed to the opening and closing of existing fractures in response to injection (Stork et al., 2015). Many of the mechanisms at play in petroleum reservoirs will also occur naturally in volcanic and geothermal systems. For example, hydraulic fracture stimulation occurs naturally as fluids move through volcanoes.

A number of studies have documented a flip of 90 degrees in φ associated with stress changes. Examples include those associated with earthquakes (Volti and Crampin, 2003), volcanic eruptions (Gerst and Savage, 2004; Savage et al., 2010; Mengesha et al., 2024) and petroleum production (Teanby et al., 2004b). There are a number of mechanisms for this, including: change in orientation of dominant stress (Gerst and Savage, 2004); a change in the relative contributions from two or more fracture systems (Teanby et al., 2004b); the influence of fluids with different compressibility, and hence a change in fracture compliance (e.g., inclusion of gas Baird et al., 2013). A more general theory of poroelasticity also attempts to explain this (Zatsepin and Crampin, 1997).

3 The eruptive history of Ontake volcano

Ontake is a complex stratovolcano located in Central Japan, on the main island of Honshū (Figure 1). In Japan volcanism is due to subduction associated with the complex interaction of four tectonic plates, and it is divided into two groups: the Eastern and Western Japan Volcanic Belts. Ontake is located at the western end of the Eastern Japan Volcanic Belt. Beneath Ontake Japan both the Pacific and Philippine Sea Plates are subducting. Standing at 3063 m, Ontake is the second highest volcano in Japan after Mount Fuji.

Ontake is underlain by a Cretaceous-Paleogene caldera complex that is crosscut by the NW-SE trending Atera fault (Kimura and Yoshida, 1999). The Atera is a left-lateral strike-slip fault associated with a nested fault system that has led to complex block rotation across the region (Kanaori et al., 1990). Secondary conjugate right-lateral faults that strike NE-SW are also prevalent. Based on 536 focal mechanisms, Terakawa et al. (2016) show that the tectonic stress regime is

characterized by strike-slip faulting with WNW-ESE compression ($\sigma_{H_{max}}$), which is oblique to the Atera fault.

Activity since the Middle Pleistocene (ca 0.78 Ma) has repeatedly built and collapsed the stratovolcano, but until recently, the volcano was thought to have been dormant for roughly 23,000 years. The first eruption of Ontake in modern times took place on the 28th October 1979, with a large (VEI 2) phreatic eruption. Since then, there have been two smaller (VEI 0) phreatic eruptions - one on 20th May 1991 and another in late March 2007. The exact date of the 2007 eruption is unknown due to a lack of visual reports, but the Japan Meteorological Agency estimate the eruption occurred between 16 and 30 March 2007 (Nakamichi et al., 2009). With little warning, a large (VEI 3) phreatic eruption on the 27th September 2014 resulted in death of at least 63 people on the mountain (Takagi and Onizawa, 2016). It was the deadliest volcanic eruption in Japan since the 1926 eruption of Tokachidake volcano (Yamaoka et al., 2016).

To help monitor unrest, a seismic network was established on the volcano in 1976. An increase in seismicity occurred before the recent eruptions (Yamaoka et al., 2016). Caudron et al. (2022) observed a sequence of correlated seismic velocity and volumetric strain changes starting 5 months before the 2014 eruption. Here we analyse seismic anisotropy using network data from the time periods of the 2007 and 2014 eruptions. Spatial variations in shallow-crustal anisotropy beneath the volcano are first assessed. We initially analyse a large volume of data at a time when there is no apparent activity in the volcano. This allows an evaluation of the background stress field within the volcanic system. We then look for perturbations in the stress field, as might be indicated through changes in the anisotropy. First, seismicity from the smaller 2007 eruption is investigated, then seismicity from the sequence associated with the larger 2014 eruption.

4 Data processing

Waveform data from shallow events beneath Mount Ontake are investigated before, during and after the 2007 event (Figure 2). The exact time of the eruption is not known, due to lack of visual confirmation, but the Japanese Meteorological Association estimate the eruption occurred sometime between the 16 to 31 March, 2007 (here, we assume the 20th March). A dataset of 539 local events (<20 km deep, but most are <10km) was recorded over 12 months in 2007, at a total of 47 stations, with an average of about 30 stations recording each event (totalling 16,645 source-receiver pairs). These consist of permanent stations established by the National Research Institute for Earth Science and Disaster Resilience (NIED), Nagoya University, the Earthquake Research Institute (ERI) and the Japan Meteorological Agency (JMA) and Nagano and Gifu prefectures.

For the 2014 sequence, the seismicity is more focused beneath the edifice of the volcano (Figure 2). We therefore analyse 94 events that occurred immediately beneath the summit of the volcano at depths less 5 km from the surface and recorded at the stations V.ONTA and V.ONTN (Figure 2). Other stations were too far away

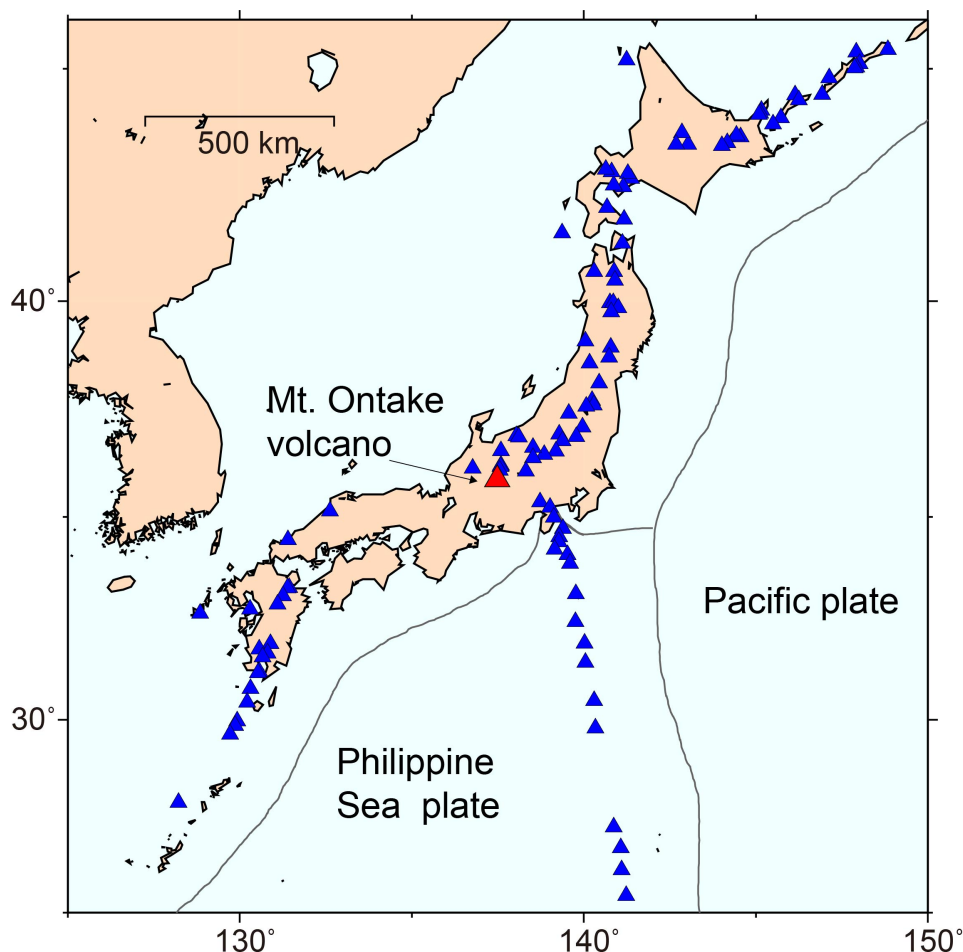


Figure 1 Location of Ontake volcano on the island of Honshū, Japan. Other regional volcanoes are shown by blue triangles, thin black lines denote plate boundaries. To the East, a less clear north-south trending boundary accommodates slow east-west convergence between the Okhotsk and Eurasian plates (not shown).

or too noisy to be considered. The emphasis is to concentrate on evidence of any change in anisotropy during the much larger 2014 eruption. These results are compared with similar events recorded at station V.ONTA during the 2007 period; note that V.ONTN did not exist in 2007.

Prior to the splitting analysis, the data are filtered between 0.5 and 3.0 Hz using a 2-pole Butterworth band-pass filter. Only raypaths that are within the S-wave window are considered for analysis, to avoid contaminations of other phases at the free surface. Booth and Crampin (1985) define the critical angle for the S-wave window as $\sin^{-1}(V_S/V_P)$. For volcanoes in general this results in a critical angle of 35° . Furthermore, we only consider waveforms with a clear S-wave onset. These restrictions reduce the 2007 dataset to 622 source-receiver pairs, which were then used for shear-wave splitting analysis. For the 2014 dataset, this results in a dataset of 96 source-receiver seismograms.

We use a semi-automated multi-window approach for evaluating shear-wave splitting, as presented by Teanby et al. (2004a) and Wuestefeld et al. (2010). This approach is based on the eigenvalue algorithm of Silver and Chan (1991). A window is defined around the S-wave arrival, and the eigenvalues of the covariance matrix of the horizontal particle motion in this window are calcu-

lated. The horizontal component seismograms are rotated by φ and time shifted by δt to remove the effects of anisotropy. If successful, this has the effect of linearising the particle motion, minimizing the second eigenvalue (λ_2) of the covariance matrix.

As we are data-rich, we only include the very best splitting results in our analyses. There are a number of criteria that need to be satisfied for a splitting measurement to be considered acceptable. Before correcting for the splitting there must be a clear separation between the fast and slow shear wave and an elliptical particle motion. Time shifting to align the fast and slow shear-wave should minimize the energy on the horizontal component that is orthogonal to the polarization of the incoming shear wave. This can be inspected visually, as this will linearise the particle motion; mathematically a linear particle motion will have a near-zero λ_2 . In practice this is done through a grid-search, where all combinations of time shifts (δt) and rotations (φ) are considered. An acceptable solution is one where there is a clear and well resolved combination of δt and φ that minimizes λ_2 . Finally, we only accept a solution where the error in δt is less than 0.04 seconds and the error in φ is less than 20 degrees.

Multiple analysis windows around the S-wave are considered and a cluster analysis is used to establish sta-

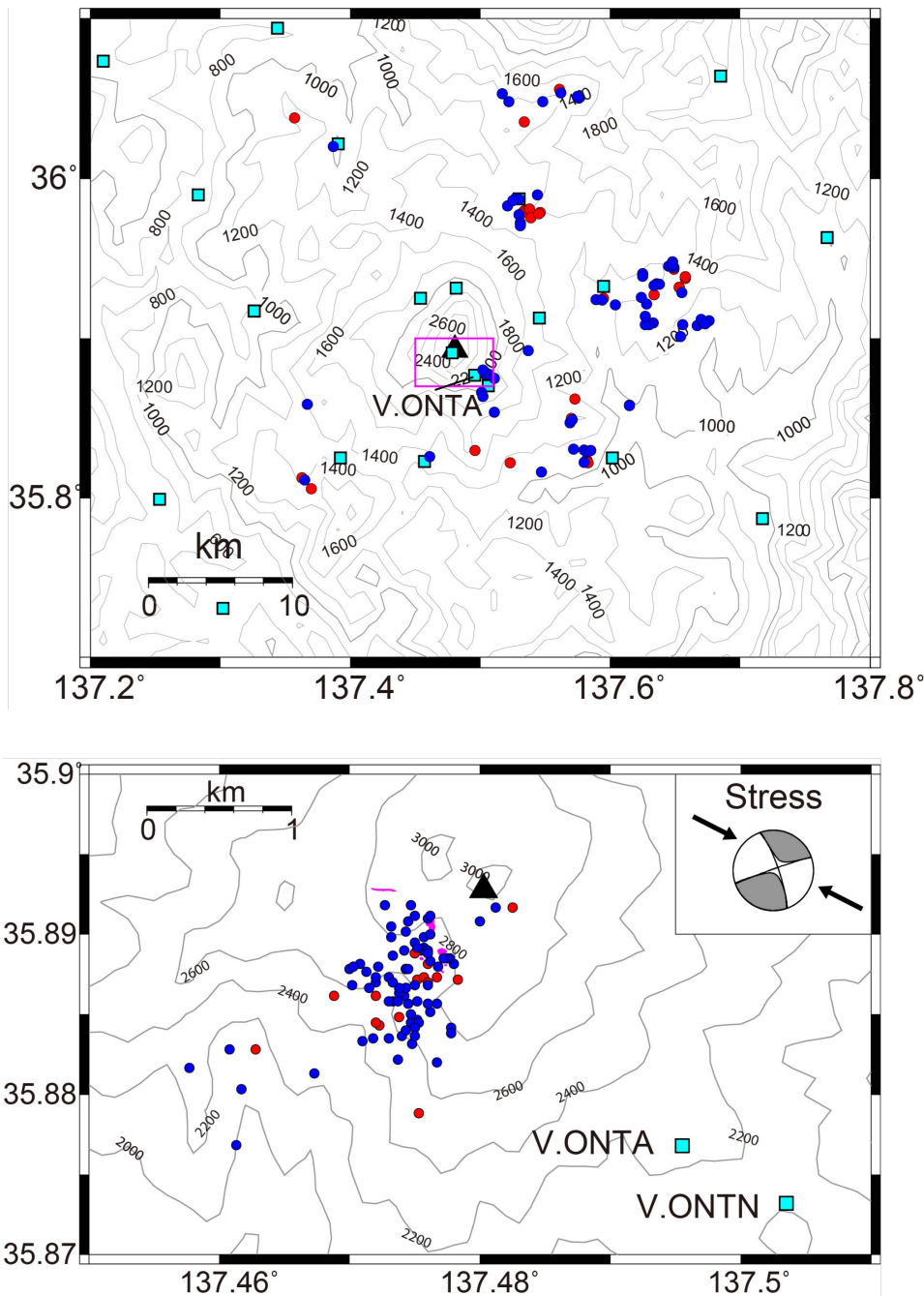


Figure 2 (top) Seismicity analysed for shear-wave splitting during the 2007 time period. Red dots indicate events before the eruption and blue dots indicate those after the eruption on the estimated date of 20th March, 2007. The black triangle indicates the peak of Mount Ontake, the cyan squares show the locations of seismic stations. Contours show topography in meters. The magenta rectangle shows the region of analysed seismicity for the 2014 sequence. (bottom) Seismicity that yielded shear-wave splitting measurements during the time period between August 2014 and April 2015. Red dots indicate events before the eruption and blue dots indicate those after the eruption on the 27th September, 2014. Inset shows a representative focal mechanism (Terakawa et al., 2016) and the direction of regional, maximum compressive principal stress. The cyan squares show the locations of seismic stations, V.ONTA and V.ONTN, and the magenta symbols show surface expressions of eruptive material. Contours show topography in meters. Note the scale differences between (a) and (b) – the seismicity in the 2014 eruption was much more focussed beneath the summit.

ble clusters of measurements. The window that corresponds to the result with the lowest error from the cluster with the lowest variance is selected. Poor quality measurements (caused by noisy data, for example) and ‘nulls’ (e.g., Wüstefeld and Bokelmann, 2007) are ignored here. We thus obtain 99 good quality measurements from the 2007 dataset and 62 for the 2014 events.

The delay time, δt , is converted into percent anisotropy along the ray path by $A = (V_S * \delta t / d) 100$, where d is the source-receiver distance and V_S is the mean shear-wave velocity (here we used $V_S = 2.0$ km/s).

We also compare these measurements with the automatic multiple filter method MFAST of Savage et al. (2010). This method is also based on the method of

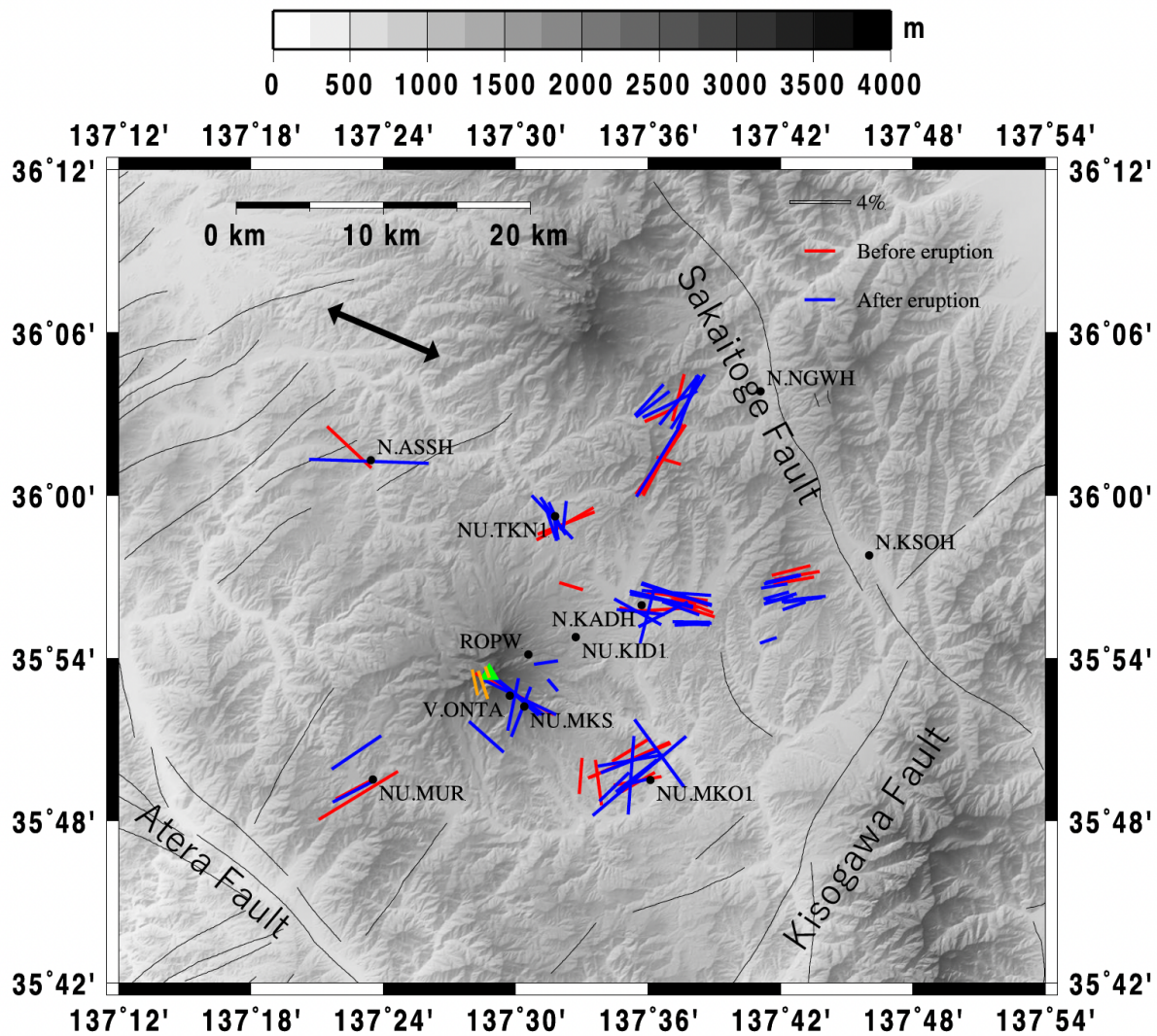


Figure 3 Shaded relief map showing faults and splitting measurements from local events in 2007. Red lines are splitting measurements from events before the late March eruption (20th March) and blue lines are measurements from after the eruption. Lines are scaled in length by percent anisotropy and their azimuth is the polarisation of the fast shear-wave, φ . Measurements are centred on ray midpoints. Thin black lines represent faults, with the Atera, Kisogawa and Sakaitoge Faults labelled. Stations recording good splitting measurements are shown by small black dots. Ontake peak is marked by the green triangle and the thick black double-arrow shows the direction of maximum horizontal stress. Orange lines show surface expressions of eruptive material.

Teanby et al. (2004a), but is extended to automatically determine the set of windows to examine based on the period of the waveform and the S-wave pick. It also tests the results over multiple filters and makes the measurement on the filtered waveform with the highest product of the signal-to-noise ratio and the bandwidth of the filter. The two methods yielded very similar results, increasing our confidence in the estimated parameters.

5 Results

shear-wave splitting results from the broad network of seismic stations across the volcano display considerable lateral variability. Figure 3 shows the individual splitting results at each of the stations for the 2007 dataset (see table S1 in supplemental information). The pattern of seismicity shows strong spatial variations. Whilst φ values for some of the stations on Ontake are roughly

parallel to the major faults and $\sigma_{H_{max}}$, many are not.

The delay time, δt , increases in the top 5 km, but then generally remains steady with greater depth (see Figure S1 in supplemental information). This is also indicated by the path averaged values of percent anisotropy. On average, the percent anisotropy decreases below 5km. These observations indicate that the majority of the anisotropy is located in the shallow part of the crust, at depths where cracks and fracture are expected to be open. This is in agreement with observations at other volcanos; e.g., Aluto (Nowacki et al., 2018), Montserrat (Baird et al., 2015), Piton de la Fournaise (Savage et al., 2015), Asama Volcano (Savage et al., 2010) and Ruapehu (Johnson et al., 2011).

Figure 3 shows the results for the period before and after the 2007 eruption at all stations. There is no evidence of a change in splitting parameters associated with the eruption. Rose diagrams for the total dataset

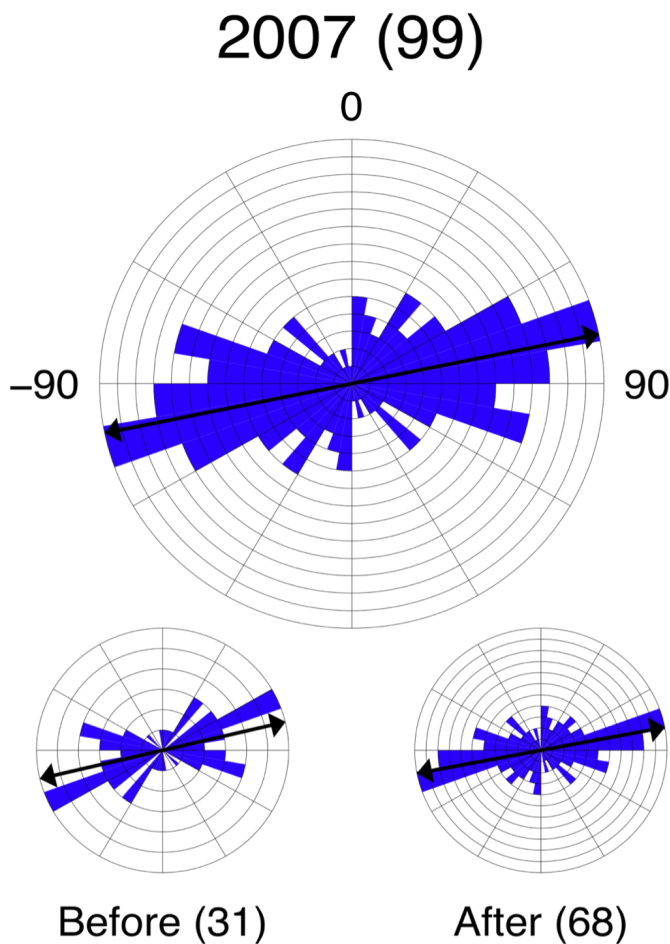


Figure 4 Rose diagrams showing distribution of φ for all measurements from local events in 2007 (top) and measurements from before (bottom left) and after (bottom right) the late March eruption. Measurements are separated into bin sectors of 10° and each grid space represents one result. The black arrows show the mean φ directions. The number of measurements is indicated in parentheses.

and the events before and after the eruption show that φ is roughly constant through 2007 (Figure 4).

In general, the entire set of results show an average φ of 78 degrees, but there is considerable variability between stations. The average delay time is 0.09 seconds, or expressed as an average percent anisotropy, 3.38%. This is roughly in agreement with values found at other volcanoes: Ruapehu – 0.1–0.17s (Miller and Savage, 2001), 0.2s (Gerst and Savage, 2004); Aluto – 0.11s (Nowacki et al., 2018); Uturuncu – 0.06s (Maher and Kendall, 2018); Montserrat – 0.2s (Baird et al., 2015); Etna – 0.05s and 0.12s (Bianco et al., 2006); Vesuvius – 0.02 (Del Pezzo et al., 2004); Okmok – 0.15s (Johnson et al., 2010); Asama – 0.11s (Savage et al., 2010).

Due to the lack of spatial coverage with the 2014 dataset, we do not look for spatial variations in splitting parameters, but rather temporal variations in shallow events beneath the summit of Ontake at stations V.ONTA and V.ONTN (Figures 5 and 6). Rose diagrams (Figure 5) show that the dominant fast polarisation direction (φ) at V.ONTA is roughly orthogonal to that observed in the 2007 sequence, but both stations clearly show two pop-

ulations in φ . Figure 6 show how the splitting parameter φ oscillates between directions parallel and perpendicular to $\sigma_{H_{max}}$. The delay time (δt) shows considerable variability, reaching a high of nearly 0.2 seconds in the days following the 2014 eruption. The increase in percent anisotropy is even more dramatic, rising from roughly 3% to 20%. Note that the 2014 events are generally shallower than those in 2007, which leads to higher estimates in the magnitude of the anisotropy.

6 Interpretation

Figure 3 shows the pattern of faulting on the volcano, with larger faults running through the middle of Ontake, oblique to $\sigma_{H_{max}}$. A secondary set of faults are oriented approximately perpendicular to this. Based on this alone, one would expect cracks in the shallow crust to remain open in the direction of $\sigma_{H_{max}}$ and to close in a direction perpendicular. Therefore, for vertically propagating shear waves, the fast shear-wave will be parallel to the direction of maximum compressive stress, parallel to the direction of open cracks, while the slow shear waves' particle motion crosses the cracks. However, the hydromagmatic system at Ontake will perturb the regional stress field. In its simplest form, a doming of the volcanic edifice would lead to a radial stress pattern, similar to the pattern of gravitational stresses due to topographical variations. Uplift would lead to local values of $\sigma_{H_{max}}$ oriented in directions radial to the edifice, as has been seen at other volcanoes (e.g., Fuji - Araragi et al., 2015). Furthermore, collapse and caldera formation could lead to ring faults and cracks oriented in a circumferential pattern around the volcano. In practice, there will be an interplay between the regional stress patterns and the local stresses exerted by volcanic processes.

The spatial distribution in the magnitude and orientation of shear wave anisotropy across the volcano shows the complicated interaction of the local stress field and the overprint of the stress field associated with the volcano (Figure 3). There is no clear radial pattern in the orientation of the fast shear-wave. Many of the stations show φ aligned with the major faults (e.g., the Artera) and $\sigma_{H_{max}}$ (e.g., V.ONTA), but others (NU.MUR) align better with secondary faults (see faults in Figure 3). Similar patterns in anisotropy controlled by faulting are observed at other volcanoes; e.g., for example, Montserrat (Baird et al., 2015), Uturuncu (Maher and Kendall, 2018) and Aluto (Nowacki et al., 2018). Such information provides insights into the state of stress in the volcano and fracture alignment at depth, which could be useful in the exploitation of geothermal reservoirs (see, for example, Elkibbi and Rial, 2005; Nowacki et al., 2018). Similar spatial variations in stress at Ontake are also interpreted from earthquake source mechanisms (Terakawa et al., 2016).

Another interesting observation is that the bulk of the anisotropy is concentrated in the upper 5 km of the volcano, likely in the hydrothermal system (see Figures S1). This is also seen at Montserrat (Baird et al., 2015), Aluto (Nowacki et al., 2018), Uturuncu (Maher and Kendall, 2018), Fuji (Araragi et al., 2015) and Ruapehu (John-

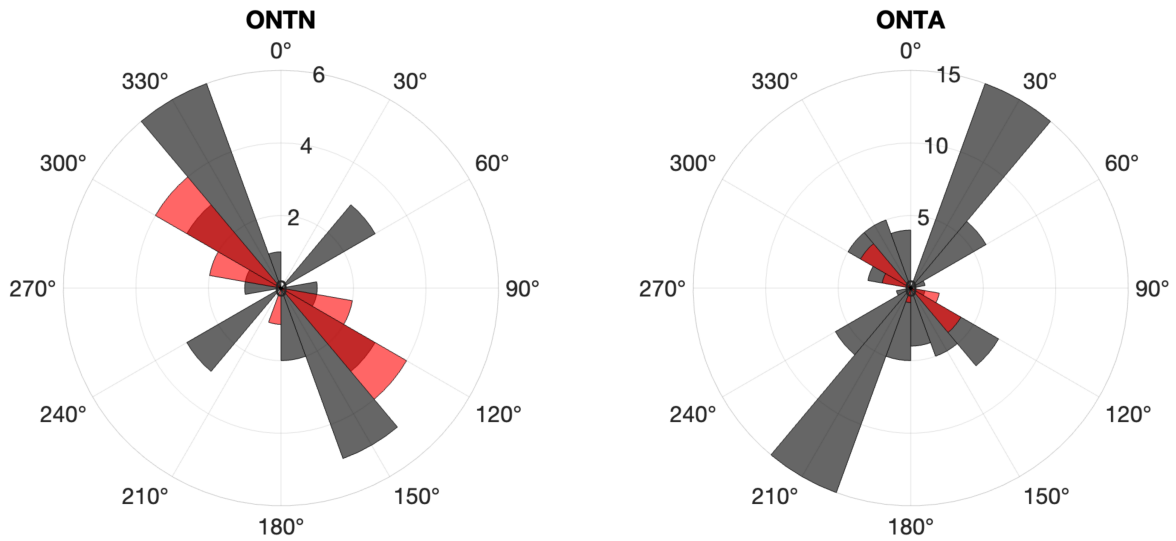


Figure 5 Rose diagrams showing distribution of φ for all measurements from local events in 2014 for the two stations V.ONTN (left) and V.ONTA (right). For comparison the red sectors show the results from V.ONTA in 2007. Figure 6 shows the variations in φ with time in 2014.

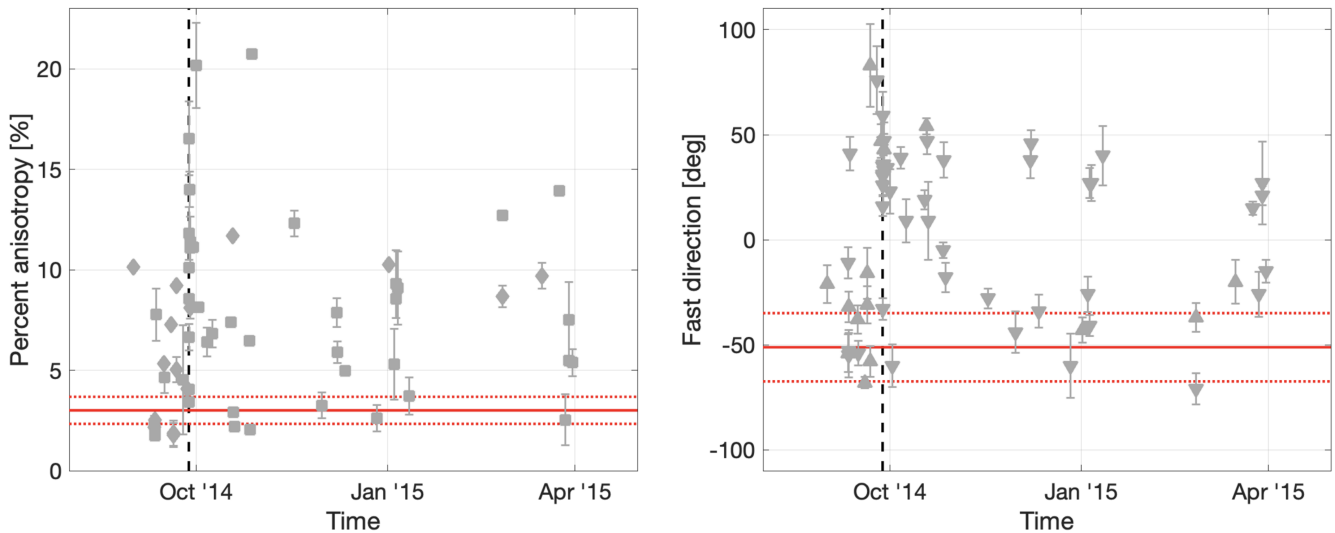


Figure 6 Splitting parameters as a function of time for the 2014 sequence. Left: delay time expressed as percent anisotropy, with squares being V.ONTA and diamonds V.ONTN) before, during and after the 2014 eruption (dashed vertical line indicates date of eruption). Right: fast shear wave polarisation, φ , in which downward-pointing triangles are from V.ONTA and upward pointing triangles are from V.ONTN. The average splitting parameters in 2007 for V.ONTA are shown as a horizontal red line, with standard deviations shown as horizontal red dashed lines. During the eruption the orientation of the fast shear wave (φ) rotates from being roughly NW-SE to a more orthogonal direction. The magnitude of the splitting (δt) increases to a peak 20% anisotropy (which corresponds to a delay time of 0.2 seconds). Figure S2 shows the splitting parameters for each station separately.

son et al., 2011). Such results are consistent with the oriented crack hypothesis for anisotropy, since cracks close rapidly with depth because of their high confining pressure (e.g., Nur, 1971). Only events that primarily sample the subcrustal mantle show significantly more anisotropy (e.g., Long and van der Hilst, 2005).

During ascent to the surface, dykes align themselves with the most energy-efficient orientation, which is roughly parallel to the direction of maximum compressive stress (e.g., Dahm, 2000; Maccaferri et al., 2010). However, the movement of magma through dyke em-

placement will locally modify the stress field. Furthermore, magma heating of phreatic fluids will lead to expansion of gases in cracks throughout the hydrothermal system. It is therefore tempting to look for temporal variations in anisotropy at times of eruption. There is no evidence of any statistically significant change in the anisotropy parameters during or after the eruption of March 2007. An exception is perhaps the station NU.TKN1, where φ changes by 80 degrees after the eruption. However, there are only 2 measurement pre-eruption, so it is difficult to be conclusive at this station.

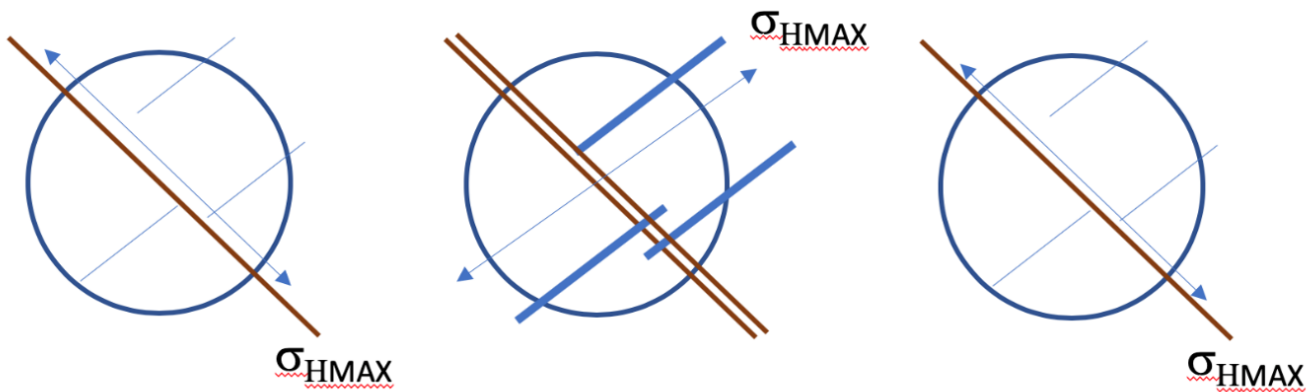


Figure 7 Interpretation of temporal variations in fracture induced anisotropy. (Left) Before the 2014 eruption the anisotropy is orientated in the direction of $\sigma_{H_{max}}$. (Middle) Immediately before and after the eruption – heat from dyke injection at depth expands fluid filled NW-SE oriented fractures, thereby dilating those with NE-SW orientations. This leads to a rotation in $\sigma_{H_{max}}$. (Right) In the months after the eruption the hydrothermal system returns to its original state.

In contrast, there are 23 measurements (7 pre- and 16 post-eruption) at station N.KADH and there is no evidence of a change in the anisotropy parameters. We conclude that this minor phreatic eruption did not perturb the background stress field enough to see a change in the anisotropy.

The 2014 eruption is accompanied by a clear change in the anisotropy parameters. Prior to the eruption, the splitting parameters at V.ONTA and V.ONTN are like those seen during the 2007 sequence at V.ONTA (Compare Figure 6 with Figures 4 and 5). Note that V.ONTN did not exist in 2007, but is located very close to V.ONTA. At these stations, which are near the peak of the volcano, the fast shear-wave polarization is parallel to $\sigma_{H_{max}}$. Roughly 1-2 days before the eruption, the magnitude of the anisotropy, or δt , shows a clear and abrupt increase of 100 ms prior to the onset of the eruption. Contemporaneously, the orientation of the fast shear-wave rotates by up to 90 degrees. In a period of over 200 days following the eruption, δt and φ decay back to the background state. This decay is not monotonic and there are brief excursions back to the eruptive state. We have some confidence that these excursions are real, as we consider only the very best splitting measurements. Furthermore, Terakawa et al. (2016) also observe transient changes in earthquake focal mechanisms of VT events. Finally, we do not see a systematic relationship between earthquake depth and fast azimuths, which if present, would have complicated interpretations in terms of time variations since the depths change after the eruption.

Cumulatively, these and other volcano observations described in the introduction span the range of anisotropy magnitudes as proposed by Crampin (1994) as the normal range of anisotropy in the crust (1.5-4.5%). Shallow crustal rocks lose shear strength and are prone to failure in cases where the anisotropy exceeds 5%. It would seem that the 2007 eruption did not exceed this critical threshold, but the 2014 eruption did.

Stix and de Moor (2018) suggest that the 2007 eruption could have been a failed eruption. Although there is evidence of a dyke injection, a wide-spread deformation signal, and LP events indicating pressurization of the hydrothermal system, the result was a minor phreatic eruption. Stix and de Moor (2018) suggest that the hydrothermal system shallowed with time since the 2007 event. Nakamichi et al. (2009) argues that the hydrothermal system was 2-3km deep in 2007, whereas Yamaoka et al. (2016) propose that the hydrothermal source was located at 1-2 km depth in 2014.

We note that there is a possibility of a more general form of anisotropy due to an azimuthal alignment of crystals, which may explain the spatial variation in anisotropy. But the temporal variation in anisotropy that we see cannot be attributed to a crystal preferred orientation (CPO) mechanism. In general, the background anisotropy could be of a more general form, but the fact that it extends no deeper than 5km, again suggests that a stress-controlled crack mechanism is dominant. Furthermore, the earthquakes in 2007 are deeper, further away from the volcano, and at different azimuths from the earthquakes in 2014. Therefore, we cannot rule out the possibility that the earthquakes in 2014 travel through a part of the crust that is particularly prone to changing stress from magmatic activity, and that there might have been a similar change in 2007 if earthquakes had come from a different region. However, we consider that scenario unlikely, and the simplest hypothesis is that the 2007 event did not change the stress field as strongly as the 2014 event.

6.1 Stress changes associated with fracture inflation

Temporal changes in anisotropy have been interpreted in terms of dyke injection at depth (e.g., Gerst and Savage, 2004; Roman et al., 2011; Savage et al., 2010, 2015). In Hawaii, changes in splitting fast polarisations that correlated with changes in increased SO_2 emissions and

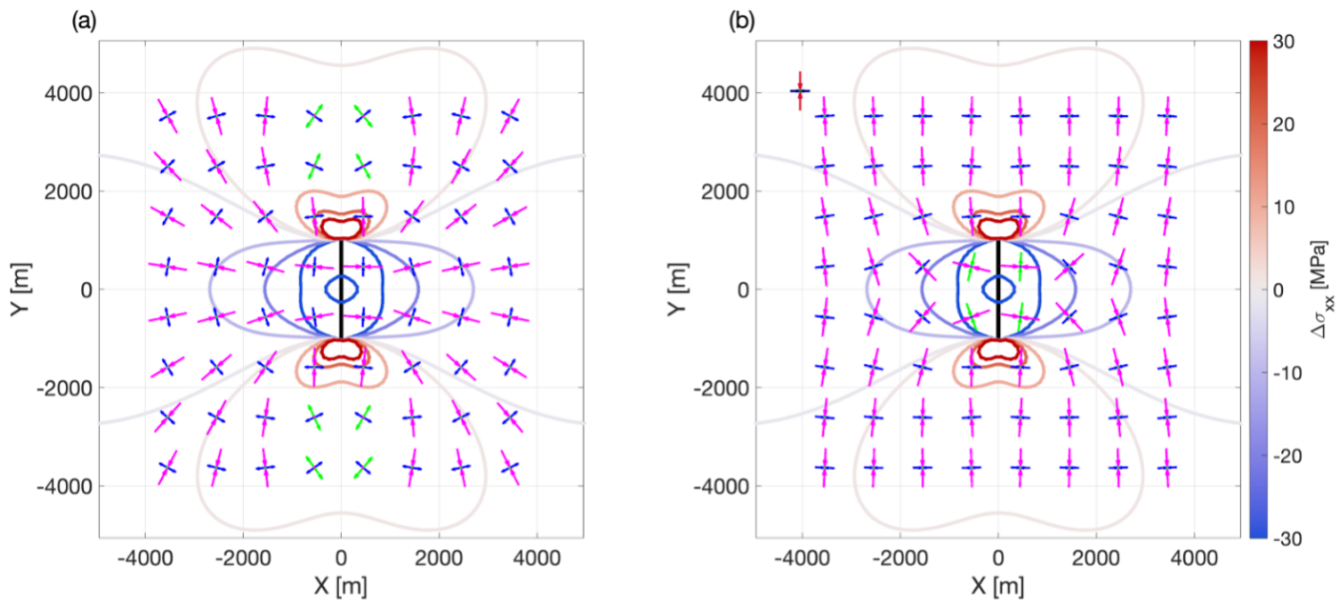


Figure 8 Map view of the changes in the orientation of the principal stresses produced by modelling the opening of a 2 km long by 2 m wide patch of fractures with a shear modulus of 32 GPa and a Poisson's ratio of 0.25 (as in [Toda et al., 2005](#); [Roman et al., 2011](#)). The patch is shown by the black line trending along the y axis, whilst the principal stress orientations are shown by the different coloured arrows: magenta for σ_1 ; green for σ_2 ; and blue for σ_3 . Contours for changes in the σ_{xx} of the stress tensor are also shown at ± 1 , ± 10 , ± 20 , and ± 30 MPa. Stress orientations and contours are plotted at the depth of the centre of the opening dike. (a) shows the changes in the orientations with no background stress state, and (b) shows when the changes in stress are applied to a strike-slip background stress, with $\sigma_1 = S_{H_{max}} = 50$ MPa, $\sigma_2 = S_V = 45$ MPa, $\sigma_3 = S_{H_{min}} = 40$ MPa, and σ_1 oriented along the y-axis.

decreasing V_p/V_s ratios were considered to be caused by changes in gas content ([Johnson and Poland, 2013](#)). At Ontake, the anisotropy is in the shallow hydrothermal system and the eruption is phreatic in nature. Here we interpret the temporal change as being due to basal heating of the hydrothermal system, which leads to an expansion of gas and liquids in a fracture network. The dominant fractures aligned with $\sigma_{H_{max}}$ dilate, thereby changing the local stress field and opening a perpendicularly oriented set of secondary fractures ([Figure 7](#)). This leads to a rotation in the orientation of the fast shear-wave and an increase in the magnitude of the anisotropy as more fractures are opened.

We test whether cracks may be changing from fluid-filled to liquid-filled by examining the ratio of P- to S-velocity, using the [Nur \(1972\)](#) relation of $T_S/T_P = V_P/V_S$, where T_S and T_P are the travel times of the S and P waves, respectively. For V.ONTA V_p/V_s was on average 1.78 ± 0.05 (95% conf interval) pre-eruption and 2.06 ± 0.04 post-eruption. For V.ONTN it was 1.8 ± 0.04 pre-eruption and 2.05 ± 0.04 post-eruption. The increase in V_p/V_s after eruption could be because either gas-filled cracks were becoming filled with liquid, or liquid-filled cracks were becoming more numerous, which we think is the most likely scenario since it fits with the same hypothesis as for increasing delay times.

We demonstrate this stress rotation using the code PSCMP of [Wang et al. \(2006\)](#). This uses the analytical [Okada \(1992\)](#) solutions to calculate the strain field resulting from the tensile opening of a planar patch in a homogenous elastic half-space. This can also be thought of in terms of a zone of dilating fractures, cre-

ating a region of tensile opening. For a given shear modulus and Poisson's ratio (or equivalently, Lamé parameters), the change in the stress tensor in three dimensions is computed. This stress change can then be added onto a background stress state to examine the rotation of the principal stress in a pre-existing stress field due to an area of tensile opening in the rock mass.

In [Figure 8](#), we show the directions of the principal stresses at a range of distances from a modelled square tensile opening patch. The dimensions of the patch follow the modelling approach of [Savage et al. \(2010\)](#) and [Roman et al. \(2011\)](#). [Figure 8a](#) shows the rotation of stress state assuming no background stress field (as in [Roman et al., 2011](#)), whilst [Figure 8b](#) shows the rotation when the stress change is applied to a pre-existing strike-slip background stress field (as in [Savage et al., 2010](#)), with the background maximum stress (σ_1) oriented parallel to the trend of the patch. Around a zone of tensile opening rock, the stress field can rotate significantly, with a noticeable deviation from the background stress state within around two source lengths. The strike slip field rotates such that the σ_1 direction is oriented perpendicular to the trend of the opening plane. The rotation of σ_1 combined with an increase in the pore pressure would allow for fractures oriented perpendicularly to the opening dike to dilate, and thus change the observed fast direction. [Figure 8b](#) also shows that more complex rotations occur in the near field (within one source length), with the intermediate stress (σ_2) becoming the minimum horizontal stress, and the minimum stress (σ_3) becoming the vertical stress. This would indicate a shift in the faulting

style that would be expected near to the zone of tensile opening, from strike-slip to reverse faulting.

6.2 Other indications of temporal change

From GNSS observation, there is a significant deformation attributed to magma intrusion and inflation associated with VT swarm prior to the 2007 Ontake eruption (Nakamichi et al., 2009), while there is no significant widespread deformation prior to the 2014 Ontake eruption (Takagi and Onizawa, 2016). This suggests a deeper origin of the signal for the 2007 event. Zhang and Wen (2015) observe 3 times more earthquakes during the 2007 eruption than the 2014 eruption.

However, there are other indications of change during the 2014 eruption. The volcanic tremors that began 11 min before the eruption were followed by rapid inflation of the edifice 4 min later (Kaneko et al., 2016). The VT seismicity before the 2014 eruption increased in the three previous weeks and reached a peak on a day two weeks before the eruption. The seismic b-values increased from 1.2 to 1.7 during this period and then declined to 0.8 just before the eruption (Kato et al., 2015). Terakawa et al. (2016) observe changes in focal mechanisms. On a longer time scale, Caudron et al. (2022) observed changes in seismic velocities, which they attributed to changes in volumetric strain occurring in the period of 5 months before the eruption. In contrast, the 2007 eruption showed an increase in VT seismicity a few months before the eruption, and a VLP event was interpreted in terms of the release of gas into the hydrothermal system (Nakamichi et al., 2009). Using levelling methods, uplift over a few years preceded both eruptions, suggesting magma intrusion into a shallow system (Murase et al., 2016).

Cumulatively, the evidence is that the origin of the 2007 event was a deeper magma intrusion, whilst the 2014 event was due to deformation in a shallower hydrothermal system. The former led to a much less significant event. This is an agreement of the assessment of Stix and de Moor (2018) that the 2007 event could be considered a failed eruption.

7 Conclusions

Observations of shear-wave splitting studied at 12 stations across Ontake volcano provide insights into the spatial and temporal variations in stress-induced anisotropy. The results reveal a complicated pattern of anisotropy indicating that the volcano perturbs the local stress field, leading to secondary crack and fracture populations. The minor phreatic eruption in 2007 showed little evidence of changes in splitting parameters during this eruption. In contrast, the much larger eruption of 2014 shows clear temporal changes in splitting parameters in the months following the eruption. The average background magnitude of anisotropy, as described by the delay time between the fast and slow shear wave, doubles from 0.09s to nearly 0.2 second at the onset of the 2014 eruption, but the percent anisotropy impressively rises from roughly 3% to 20%.

Contemporaneously, the polarisation of the fast shear-wave, φ , rotates towards $\sigma_{H_{max}}$. These observations are interpreted in terms of basal heating of the hydrothermal system, which perturbs the stress field, dilating secondary fractures aligned perpendicular to $\sigma_{H_{max}}$.

The observation of a temporal change in anisotropy during the 2014 eruption of Ontake is one of only a few documented examples of anisotropy changes during a volcanic eruption. The fact that there is no change observed during the 2007 eruption suggests that there is a critical stress threshold that must be overcome, which may be why a change in shear-wave splitting is not always observed. Based on this and other lines of evidence, it appears that this 2007 event was associated with deeper magma movement, whereas the more dangerous 2014 event was associated with the shallow hydrothermal system.

Once a critical fracture density is overcome, the rock loses shear strength, thus permitting an eruption. These observations suggest that observations of shear-wave splitting serve as an important indicator of stress changes and precursors of significant eruptions. Shear-wave splitting measurements can be automated (e.g., Wuestefeld et al., 2010; Savage et al., 2010) – source location is the time limiting step, but recent advances with machine learning suggest that real-time monitoring is a realistic aspiration (Lapins et al., 2021). As such, seismic anisotropy is a seismic attribute that could be incorporated into the probabilistic eruption forecasting toolbox.

Acknowledgements

J-M. Kendall gratefully acknowledges support from the Nagoya University and Prof. Simon Wallis for a Visiting Professorship. J-M. Kendall and Tom Kettley were partly funded by a grant from the Natural Environment Research Council (NE/R018006/1) and from the University of Oxford through the Oxford Net Zero programme. Martha Savage was partially supported for this work from a Meaker Fellowship from the University of Bristol, from a Visiting Lecturer appointment at Earthquake Research Institute, University of Tokyo and from New Zealand's Resilience to Nature's Challenges Grant NSC06. We are grateful for constructive reviews from Luca De Siena and the handling editor Nicola Piana Agostinetti. We thank Théa Ragon for copy-editing and Gareth Funning for production editing.

Data and code availability

Data are archived on Zenodo at <https://doi.org/10.5281/zenodo.14598534>.

Competing interests

The authors have no competing interests.

References

Adelinet, M., Dorbath, C., Calò, M., Dorbath, L., and Le Ravalec, M. Crack Features and Shear-Wave Splitting Associated with Frac-

- ture Extension during Hydraulic Stimulation of the Geothermal Reservoir in Soultz-sous-Forêts. *Oil & Gas Science and Technology – Revue d' IFP Energies nouvelles*, 71(3):39, Sept. 2015. doi: 10.2516/ogst/2015023.
- Al-Harrasi, O., Al-Anboori, A., Wüstefeld, A., and Kendall, J.-M. Seismic anisotropy in a hydrocarbon field estimated from microseismic data. *Geophysical Prospecting*, 59(2):227 – 243, Aug. 2010. doi: 10.1111/j.1365-2478.2010.00915.x.
- Araragi, K. R., Savage, M. K., Ohminato, T., and Aoki, Y. Seismic anisotropy of the upper crust around Mount Fuji, Japan. *Journal of Geophysical Research: Solid Earth*, 120(4):2739 – 2751, Apr. 2015. doi: 10.1002/2014jb011554.
- Baird, A. F., Kendall, J.-M., Verdon, J. P., Wuestefeld, A., Noble, T. E., Li, Y., Dutko, M., and Fisher, Q. J. Monitoring increases in fracture connectivity during hydraulic stimulations from temporal variations in shear wave splitting polarization. *Geophysical Journal International*, 195(2):1120 – 1131, Aug. 2013. doi: 10.1093/gji/ggt274.
- Baird, A. F., Kendall, J.-M., Sparks, R. S. J., and Baptie, B. Transtensional deformation of Montserrat revealed by shear wave splitting. *Earth and Planetary Science Letters*, 425:179 – 186, Sept. 2015. doi: 10.1016/j.epsl.2015.06.006.
- Baird, A. F., Kendall, J. M., Fisher, Q. J., and Budge, J. The Role of Texture, Cracks, and Fractures in Highly Anisotropic Shales. *Journal of Geophysical Research: Solid Earth*, 122(12), Dec. 2017. doi: 10.1002/2017jb014710.
- Bianco, F., Scarfi, L., Del Pezzo, E., and Patanè, D. Shear wave splitting changes associated with the 2001 volcanic eruption on Mt Etna. *Geophysical Journal International*, 167(2):959 – 967, Nov. 2006. doi: 10.1111/j.1365-246x.2006.03152.x.
- Booth, D. C. and Crampin, S. Shear-wave polarizations on a curved wavefront at an isotropic free surface. *Geophysical Journal International*, 83(1):31 – 45, Oct. 1985. doi: 10.1111/j.1365-246x.1985.tb05154.x.
- Caudron, C., Aoki, Y., Lecocq, T., De Plaen, R., Soubestre, J., Mordret, A., Seydoux, L., and Terakawa, T. Hidden pressurized fluids prior to the 2014 phreatic eruption at Mt Ontake. *Nature Communications*, 13(1), Oct. 2022. doi: 10.1038/s41467-022-32252-w.
- Chapman, M. Frequency-dependent anisotropy due to meso-scale fractures in the presence of equant porosity. *Geophysical Journal International*, 83(1):31 – 45, Oct. 1985. doi: 10.1046/j.1365-2478.2003.00384.x.
- Chouet, B. A. Long-period volcano seismicity: its source and use in eruption forecasting. *Nature*, 380(6572):309 – 316, Mar. 1996. doi: 10.1038/380309a0.
- Chouet, B. A. and Matoza, R. S. A multi-decadal view of seismic methods for detecting precursors of magma movement and eruption. *Journal of Volcanology and Geothermal Research*, 252: 108 – 175, Feb. 2013. doi: 10.1016/j.jvolgeores.2012.11.013.
- Crampin, S. Effective anisotropic elastic constants for wave propagation through cracked solids. *Geophysical Journal International*, 76(1):135 – 145, Jan. 1984. doi: 10.1111/j.1365-246x.1984.tb05029.x.
- Crampin, S. The fracture criticality of crustal rocks. *Geophysical Journal International*, 118(2):428 – 438, Aug. 1994. doi: 10.1111/j.1365-246x.1994.tb03974.x.
- Dahlen, F. A. Elastic velocity anisotropy in the presence of an anisotropic initial stress. *Bulletin of the Seismological Society of America*, 62(5):1183 – 1193, Oct. 1972. doi: 10.1785/bssa0620051183.
- Dahm, T. Numerical simulations of the propagation path and the arrest of fluid-filled fractures in the Earth. *Geophysical Journal International*, 141(3):623 – 638, June 2000. doi: 10.1046/j.1365-246x.2000.00102.x.
- De Meersman, K., Kendall, J.-M., and van der Baan, M. The 1998 Valhall microseismic data set: An integrated study of relocated sources, seismic multiplets, and S-wave splitting. *Geophysics*, 74(5):B183 – B195, Sept. 2009. doi: 10.1190/1.3205028.
- De Siena, L., Thomas, C., Waite, G. P., Moran, S. C., and Klemme, S. Attenuation and scattering tomography of the deep plumbing system of Mount St. Helens. *Journal of Geophysical Research: Solid Earth*, 119(11):8223 – 8238, Nov. 2014. doi: 10.1002/2014jb011372.
- Del Pezzo, E., Bianco, F., Petrosino, S., and Saccorotti, G. Changes in the Coda Decay Rate and Shear-Wave Splitting Parameters Associated with Seismic Swarms at Mt. Vesuvius, Italy. *Bulletin of the Seismological Society of America*, 94(2):439 – 452, Apr. 2004. doi: 10.1785/0120030141.
- Elkibbi, M. and Rial, J. A. The Geysers geothermal field: results from shear-wave splitting analysis in a fractured reservoir. *Geophysical Journal International*, 162(3):1024 – 1035, Sept. 2005. doi: 10.1111/j.1365-246x.2005.02698.x.
- Gerst, A. and Savage, M. K. Seismic Anisotropy Beneath Ruapehu Volcano: A Possible Eruption Forecasting Tool. *Science*, 306(5701):1543 – 1547, Nov. 2004. doi: 10.1126/science.1103445.
- González, M. and Munguía, L. Seismic Anisotropy Observations in the Mexicali Valley, Baja California, México. *pure and applied geophysics*, 160(12):2257 – 2278, Dec. 2003. doi: 10.1007/s00024-003-2393-1.
- Hamling, I. J. and Kilgour, G. Goldilocks conditions required for earthquakes to trigger basaltic eruptions: Evidence from the 2015 Ambrym eruption. *Science Advances*, 6(14), Apr. 2020. doi: 10.1126/sciadv.aaz5261.
- Hudson, T. S., Kendall, J. M., Blundy, J. D., Pritchard, M. E., MacQueen, P., Wei, S. S., Gottsmann, J. H., and Lapins, S. Hydrothermal Fluids and Where to Find Them: Using Seismic Attenuation and Anisotropy to Map Fluids Beneath Uturuncu Volcano, Bolivia. *Geophysical Research Letters*, 50(5), Feb. 2023. doi: 10.1029/2022gl100974.
- Illsley-Kemp, F., Savage, M. K., Keir, D., Hirschberg, H. P., Bull, J. M., Gernon, T. M., Hammond, J. O., Kendall, J.-M., Ayele, A., and Goitom, B. Extension and stress during continental breakup: Seismic anisotropy of the crust in Northern Afar. *Earth and Planetary Science Letters*, 477:41 – 51, Nov. 2017. doi: 10.1016/j.epsl.2017.08.014.
- Johnson, J. H. and Poland, M. P. Seismic detection of increased degassing before Kilauea's 2008 summit explosion. *Nature Communications*, 4(1), Apr. 2013. doi: 10.1038/ncomms2703.
- Johnson, J. H., Prejean, S., Savage, M. K., and Townend, J. Anisotropy, repeating earthquakes, and seismicity associated with the 2008 eruption of Okmok volcano, Alaska. *Journal of Geophysical Research: Solid Earth*, 115(B9), Sept. 2010. doi: 10.1029/2009jb006991.
- Johnson, J. H., Savage, M. K., and Townend, J. Distinguishing between stress-induced and structural anisotropy at Mount Ruapehu volcano, New Zealand. *Journal of Geophysical Research*, 116(B12), Dec. 2011. doi: 10.1029/2011jb008308.
- Jones, G., Kendall, J., Bastow, I., Raymer, D., and Wuestefeld, A. Characterization of fractures and faults: a multi-component passive microseismic study from the Ekofisk reservoir. *Geophysical Prospecting*, 62(4):779 – 796, May 2014. doi: 10.1111/1365-2478.12139.
- Kanaori, Y., Endo, Y., Yairi, K., and Kawakami, S.-I. A nested fault system with block rotation caused by left-lateral faulting: the Neodani and Atera faults, central Japan. *Tectonophysics*, 177(4):401 – 418, June 1990. doi: 10.1016/0040-1951(90)90398-r.

- Kaneko, T., Maeno, F., and Nakada, S. 2014 Mount Ontake eruption: characteristics of the phreatic eruption as inferred from aerial observations. *Earth, Planets and Space*, 68(1), May 2016. doi: 10.1186/s40623-016-0452-y.
- Kato, A., Terakawa, T., Yamanaka, Y., Maeda, Y., Horikawa, S., Matsuhiko, K., and Okuda, T. Preparatory and precursory processes leading up to the 2014 phreatic eruption of Mount Ontake, Japan. *Earth, Planets and Space*, 67(1), July 2015. doi: 10.1186/s40623-015-0288-x.
- Kendall, J.-M. *Seismic anisotropy in the boundary layers of the Earth's mantle, Earth's Deep Interior: Mineral Physics and Tomography from the Atomic to the Global Scale*, page 133 – 159. American Geophysical Union, 2000. doi: 10.1029/gm117p0133.
- Kendall, J.-M., Fisher, Q. J., Crump, S. C., Maddock, J., Carter, A., Hall, S. A., Wookey, J., Valcke, S. L. A., Casey, M., Lloyd, G., and Ismail, W. B. Seismic anisotropy as an indicator of reservoir quality in siliciclastic rocks. *Geological Society, London, Special Publications*, 292(1):123 – 136, Jan. 2007. doi: 10.1144/sp292.7.
- Kimura, J. and Yoshida, T. Magma plumbing system beneath Ontake Volcano, central Japan. *Island Arc*, 8(1):1 – 29, Mar. 1999. doi: 10.1046/j.1440-1738.1999.00219.x.
- Koulakov, I., Maksotova, G., Jaxybulatov, K., Kasatkina, E., Shapiro, N. M., Luehr, B., El Khrepy, S., and Al-Arifi, N. Structure of magma reservoirs beneath Merapi and surrounding volcanic centers of Central Java modeled from ambient noise tomography. *Geochemistry, Geophysics, Geosystems*, 17(10):4195 – 4211, Oct. 2016. doi: 10.1002/2016gc006442.
- Lapins, S., Roman, D. C., Rougier, J., De Angelis, S., Cashman, K. V., and Kendall, J.-M. An examination of the continuous wavelet transform for volcano-seismic spectral analysis. *Journal of Volcanology and Geothermal Research*, 389:106728, Jan. 2020. doi: 10.1016/j.jvolgeores.2019.106728.
- Lapins, S., Goitom, B., Kendall, J., Werner, M. J., Cashman, K. V., and Hammond, J. O. S. A Little Data Goes a Long Way: Automating Seismic Phase Arrival Picking at Nabro Volcano With Transfer Learning. *Journal of Geophysical Research: Solid Earth*, 126(7), July 2021. doi: 10.1029/2021jb021910.
- Long, M. D. and van der Hilst, R. D. Upper mantle anisotropy beneath Japan from shear wave splitting. *Physics of the Earth and Planetary Interiors*, 151(3 – 4):206 – 222, Aug. 2005. doi: 10.1016/j.pepi.2005.03.003.
- Maccaferri, F., Bonafede, M., and Rivalta, E. A numerical model of dyke propagation in layered elastic media. *Geophysical Journal International*, 180(3):1107 – 1123, Mar. 2010. doi: 10.1111/j.1365-246x.2009.04495.x.
- Maher, S. and Kendall, J.-M. Crustal anisotropy and state of stress at Uturuncu Volcano, Bolivia, from shear-wave splitting measurements and magnitude – frequency distributions in seismicity. *Earth and Planetary Science Letters*, 495:38 – 49, Aug. 2018. doi: 10.1016/j.epsl.2018.04.060.
- Malfante, M., Dalla Mura, M., Metaxian, J.-P., Mars, J. I., Macedo, O., and Inza, A. Machine Learning for Volcano-Seismic Signals: Challenges and Perspectives. *IEEE Signal Processing Magazine*, 35(2):20 – 30, Mar. 2018. doi: 10.1109/msp.2017.2779166.
- Manga, M. and Brodsky, E. SEISMIC TRIGGERING OF ERUPTIONS IN THE FAR FIELD: Volcanoes and Geysers. *Annual Review of Earth and Planetary Sciences*, 34(1):263 – 291, May 2006. doi: 10.1146/annurev.earth.34.031405.125125.
- McNutt, S. R. *Seismic Monitoring and Eruption Forecasting of Volcanoes: A Review of the State-of-the-Art and Case Histories*, page 99 – 146. Springer Berlin Heidelberg, 1996. doi: 10.1007/978-3-642-80087-0_3.
- McNutt, S. R. VOLCANIC SEISMOLOGY. *Annual Review of Earth and Planetary Sciences*, 33(1):461 – 491, May 2005. doi: 10.1146/annurev.earth.33.092203.122459.
- Mengesha, D. Y., Savage, M. K., Jolly, A. D., and Ebinger, C. J. Time Varying Crustal Anisotropy at Whakaari/White Island Volcano. *Geophysical Research Letters*, 51(11), June 2024. doi: 10.1029/2023gl106473.
- Miller, V. and Savage, M. Changes in Seismic Anisotropy After Volcanic Eruptions: Evidence from Mount Ruapehu. *Science*, 293(5538):2231 – 2233, Sept. 2001. doi: 10.1126/science.1063463.
- Mroczek, S., Savage, M. K., Hopp, C., and Sewell, S. M. Anisotropy as an indicator for reservoir changes: example from the Rotokawa and Ngatamariki geothermal fields, New Zealand. *Geophysical Journal International*, 220(1):1 – 17, Sept. 2019. doi: 10.1093/gji/ggz400.
- Murase, M., Kimata, F., Yamanaka, Y., Horikawa, S., Matsuhiko, K., Matsushima, T., Mori, H., Ohkura, T., Yoshikawa, S., Miyajima, R., Inoue, H., Mishima, T., Sonoda, T., Uchida, K., Yamamoto, K., and Nakamichi, H. Preparatory process preceding the 2014 eruption of Mount Ontake volcano, Japan: insights from precise leveling measurements. *Earth, Planets and Space*, 68(1), Jan. 2016. doi: 10.1186/s40623-016-0386-4.
- Nakamichi, H., Kumagai, H., Nakano, M., Okubo, M., Kimata, F., Ito, Y., and Obara, K. Source mechanism of a very-long-period event at Mt Ontake, central Japan: Response of a hydrothermal system to magma intrusion beneath the summit. *Journal of Volcanology and Geothermal Research*, 187(3 – 4):167 – 177, Nov. 2009. doi: 10.1016/j.jvolgeores.2009.09.006.
- Neuberg, J. Characteristics and causes of shallow seismicity in andesite volcanoes. *Philosophical Transactions of the Royal Society of London. Series A: Mathematical, Physical and Engineering Sciences*, 358(1770):1533 – 1546, May 2000. doi: 10.1098/rsta.2000.0602.
- Nowacki, A., Wilks, M., Kendall, J.-M., Biggs, J., and Ayele, A. Characterising hydrothermal fluid pathways beneath Aluto volcano, Main Ethiopian Rift, using shear wave splitting. *Journal of Volcanology and Geothermal Research*, 356:331 – 341, May 2018. doi: 10.1016/j.jvolgeores.2018.03.023.
- Nur, A. Effects of stress on velocity anisotropy in rocks with cracks. *Journal of Geophysical Research*, 76(8):2022 – 2034, Mar. 1971. doi: 10.1029/jb076i008p02022.
- Nur, A. Dilatancy, pore fluids, and premonitory variations of ts/tp travel times. *Bulletin of the Seismological Society of America*, 62(5):1217 – 1222, Oct. 1972. doi: 10.1785/bssa0620051217.
- Nur, A. and Simmons, G. Stress-induced velocity anisotropy in rock: An experimental study. *Journal of Geophysical Research*, 74(27):6667 – 6674, Dec. 1969. doi: 10.1029/jb074i027p06667.
- Okada, Y. Internal deformation due to shear and tensile faults in a half-space. *Bulletin of the Seismological Society of America*, 82(2):1018 – 1040, Apr. 1992. doi: 10.1785/bssa0820021018.
- Petersen, T., Gledhill, K., Chadwick, M., Gale, N. H., and Ristau, J. The New Zealand National Seismograph Network. *Seismological Research Letters*, 82(1):9 – 20, Jan. 2011. doi: 10.1785/gssrl.82.1.9.
- Roman, D., Moran, S., Power, J., and Cashman, K. Temporal and Spatial Variation of Local Stress Fields before and after the 1992 Eruptions of Crater Peak Vent, Mount Spurr Volcano, Alaska. *Bulletin of the Seismological Society of America*, 94(6):2366 – 2379, Dec. 2004. doi: 10.1785/0120030259.
- Roman, D. C., Savage, M. K., Arnold, R., Latchman, J. L., and De Angelis, S. Analysis and forward modeling of seismic anisotropy during the ongoing eruption of the Soufrière Hills Volcano, Montserrat, 1996 – 2007. *Journal of Geophysical Research*, 116(B3), Mar. 2011. doi: 10.1029/2010jb007667.
- Savage, M., Ohminato, T., Aoki, Y., Tsuji, H., and Greve, S.

- Stress magnitude and its temporal variation at Mt. Asama Volcano, Japan, from seismic anisotropy and GPS. *Earth and Planetary Science Letters*, 290:403 – 414, 2010. doi: 10.1016/j.epsl.2009.12.037.
- Savage, M. K. Seismic anisotropy and mantle deformation: What have we learned from shear wave splitting? *Reviews of Geophysics*, 37(1):65 – 106, Feb. 1999. doi: 10.1029/98rg02075.
- Savage, M. K., Ferrazzini, V., Peltier, A., Rivemale, E., Mayor, J., Schmid, A., Brenguier, F., Massin, F., Got, J., Battaglia, J., DiMuro, A., Staudacher, T., Rivet, D., Taisne, B., and Shelley, A. Seismic anisotropy and its precursory change before eruptions at Piton de la Fournaise volcano, La Réunion. *Journal of Geophysical Research: Solid Earth*, 120(5):3430 – 3458, May 2015. doi: 10.1002/2014jb011665.
- Schoenberg, M. and Sayers, C. M. Seismic anisotropy of fractured rock. *Geophysics*, 60(1):204 – 211, Jan. 1995. doi: 10.1190/1.1443748.
- Silver, P. G. and Chan, W. W. Shear wave splitting and subcontinental mantle deformation. *Journal of Geophysical Research: Solid Earth*, 96(B10):16429 – 16454, Sept. 1991. doi: 10.1029/91jb00899.
- Sparks, R. S. J. and Aspinall, W. P. *Volcanic activity: Frontiers and challenges in forecasting, prediction and risk assessment*, page 359 – 373. American Geophysical Union, 2004. doi: 10.1029/150gm28.
- Stix, J. and de Moor, J. M. Understanding and forecasting phreatic eruptions driven by magmatic degassing. *Earth, Planets and Space*, 70(1), May 2018. doi: 10.1186/s40623-018-0855-z.
- Stork, A. L., Verdon, J. P., and Kendall, J.-M. The microseismic response at the In Salah Carbon Capture and Storage (CCS) site. *International Journal of Greenhouse Gas Control*, 32:159 – 171, Jan. 2015. doi: 10.1016/j.ijggc.2014.11.014.
- Takagi, A. and Onizawa, S. Shallow pressure sources associated with the 2007 and 2014 phreatic eruptions of Mt. Ontake, Japan. *Earth, Planets and Space*, 68(1), July 2016. doi: 10.1186/s40623-016-0515-0.
- Teanby, N., Kendall, J., and Baan, M. Automation of Shear-Wave Splitting Measurements using Cluster Analysis. *Bulletin of the Seismological Society of America*, 94(2):453 – 463, Apr. 2004a. doi: 10.1785/0120030123.
- Teanby, N., Kendall, J.-M., Jones, R. H., and Barkved, O. Stress-induced temporal variations in seismic anisotropy observed in microseismic data. *Geophysical Journal International*, 156(3): 459 – 466, Mar. 2004b. doi: 10.1111/j.1365-246x.2004.02212.x.
- Terakawa, T., Kato, A., Yamanaka, Y., Maeda, Y., Horikawa, S., Matsuhira, K., and Okuda, T. Monitoring eruption activity using temporal stress changes at Mount Ontake volcano. *Nature Communications*, 7(1), Feb. 2016. doi: 10.1038/ncomms10797.
- Toda, S., Stein, R. S., Richards-Dinger, K., and Bozkurt, S. B. Forecasting the evolution of seismicity in southern California: Animations built on earthquake stress transfer. *Journal of Geophysical Research: Solid Earth*, 110(B5), May 2005. doi: 10.1029/2004jb003415.
- Tsvankin, I., Gaiser, J., Grechka, V., van der Baan, M., and Thomsen, L. Seismic anisotropy in exploration and reservoir characterization: An overview. *Geophysics*, 75(5):75A15–75A29, Sept. 2010. doi: 10.1190/1.3481775.
- Verdon, J. P., Kendall, J.-M., and Wüstefeld, A. Imaging fractures and sedimentary fabrics using shear wave splitting measurements made on passive seismic data. *Geophysical Journal International*, 179(2):1245 – 1254, Nov. 2009. doi: 10.1111/j.1365-246x.2009.04347.x.
- Volti, T. and Crampin, S. A four-year study of shear-wave splitting in Iceland: 2. Temporal changes before earthquakes and volcanic eruptions. *Geological Society, London, Special Publications*, 212 (1):135 – 149, Jan. 2003. doi: 10.1144/gsl.sp.2003.212.01.09.
- Wang, R., Lorenzo-Martín, F., and Roth, F. PSGRN/PSCMP—a new code for calculating co- and post-seismic deformation, geoid and gravity changes based on the viscoelastic-gravitational displacement theory. *Computers & Geosciences*, 32(4):527 – 541, May 2006. doi: 10.1016/j.cageo.2005.08.006.
- Wegler, U., Lühr, B., Snieder, R., and Ratdomopurbo, A. Increase of shear wave velocity before the 1998 eruption of Merapi volcano (Indonesia). *Geophysical Research Letters*, 33(9), May 2006. doi: 10.1029/2006gl025928.
- Wuestefeld, A., Al-Harrasi, O., Verdon, J. P., Wookey, J., and Kendall, J. M. A strategy for automated analysis of passive microseismic data to image seismic anisotropy and fracture characteristics. *Geophysical Prospecting*, 58(5):755 – 773, Aug. 2010. doi: 10.1111/j.1365-2478.2010.00891.x.
- Wuestefeld, A., Verdon, J. P., Kendall, J.-M., Rutledge, J., Clarke, H., and Wookey, J. Inferring rock fracture evolution during reservoir stimulation from seismic anisotropy. *Geophysics*, 76(6): WC157 – WC166, Nov. 2011. doi: 10.1190/geo2011-0057.1.
- Yamaoka, K., Geshi, N., Hashimoto, T., Ingebritsen, S. E., and Oikawa, T. Special issue “The phreatic eruption of Mt. Ontake volcano in 2014” . *Earth, Planets and Space*, 68(1), Nov. 2016. doi: 10.1186/s40623-016-0548-4.
- Zatsepin, S. V. and Crampin, S. Modelling the compliance of crustal rock - I. Response of shear-wave splitting to differential stress. *Geophysical Journal International*, 129(3):477 – 494, June 1997. doi: 10.1111/j.1365-246x.1997.tb04488.x.
- Zhang, M. and Wen, L. Earthquake characteristics before eruptions of Japan’s Ontake volcano in 2007 and 2014. *Geophysical Research Letters*, 42(17):6982 – 6988, Sept. 2015. doi: 10.1002/2015gl065165.

The article *Changes in seismic anisotropy at Ontake volcano: a tale of two eruptions* © 2025 by J.-M. Kendall is licensed under CC BY 4.0.